http://dx.doi.org/10.17159/2411-9717/2019/v119n2a12

Changes in subsidence-field surface movement in shallow-seam coal mining

by X-J. Liu* and Z-B. Cheng†

Synopsis

Intensive mining of shallow coal seams tends to result in severe subsidence of the ground surface. Surface subsidence is a complex dynamic spatiotemporal process that constantly changes as mining advances. With Liangshuijing coal mine as a case study, 3DEC numerical software was used to simulate the development of the moving subsidence field from open-off cut to full subsidence on the working face. The results demonstrate that the formation of a subsidence field is directly related to the coal seam depth H and the extent of the mine workings. Taking the advance distance of the working face as the unit of scale, the process of surface subsidence can be divided into four stages: micro-change (H/π), the development of surface subsidence ($2H/\pi$), the formation of a movement subsidence field ($3H/\pi$), and dynamic balance ($4H/\pi$). The changing movement of a subsidence field can be fully described by the characteristics of surface subsidence value, curve slope, and the inflection position. The results provide important technical support for predicting surface subsidence and the temporal–spatial evolution features of mining subsidence.

Keywords
coal seam, subsidence, surface movement, mining.

Introduction

China's coal output was about 3.52 Gt in 2017 (China National Coal Association, 2018), making it the largest coal producer in the world, accounting for almost half of total world coal production. Coal production and distribution play a vital role in the energy industry of China. However, entire overlying strata, from coal seam to surface, are disturbed as a result of long-term, high-intensity and large-scale mining, causing surface subsidence. This results in groundwater loss, surface desertification, vegetation loss, and mud-rock flows. These issues have become topics of common concern throughout society. According to related research results (Liu 2008), the area of surface subsidence caused by coal mining in China has reached about 600 000 ha, some 0.2 ha (and up to 0.42 ha) of surface subsidence for every 10 000 t of coal produced. Surface subsidence disasters not only damage buildings, water conservancy, transportation infrastructure, and farmland, but also cause adverse effects on individual and community lifestyles, environmental hygiene, and economic development. Deterioration of the ecological environment in mining areas has a long history and is very harmful (Lu, 2015).

Surface subsidence is an extremely important control index for underground excavations. Many experts and scholars have devoted resources to the research and remediation of damage caused by coal mining from the surveying, numerical simulation, mathematical, mechanical, geological, and mining engineering points of view. These studies have revealed general laws of mining subsidence (Hu, 2012). The most prominent characteristic of these is that surface subsidence has an obvious time-dependency, and may continue for several months, or even years, from the start to the end of surface movements. Since the 1970s, with the wide application of computer methods, numerical simulation has been increasingly applied in the calculation of mining subsidence and the analysis of subsidence mechanisms, and many experts and scholars have undertaken research in this field, such as Dahl and Choi (1981). The West German scholar Kratzsch (1974) summarized methods of predicting coal mining subsidence in his book 'Mining Damage and Protection'. Ma and Yang (2001) researched the spatial and temporal effects of rock movement using the discrete element method. Cui and Deng (2017) carried out a real-time displacement analysis of surface movement and deformation for the main section of a coal mine, and studied mining subsidence utilizing a rheological model.

Surface subsidence continually changes during the exploitation of a mining face;

* *State Key Laboratory of Water Resource Protection and Utilization in Coal Mining, Beijing, China.*
† *Department of Ground Engineering, School of Engineering, University of Warwick, Coventry, United Kingdom.*
 ISSN 2225-6253. Paper received Nov. 2017; revised paper received Aug. 2018.

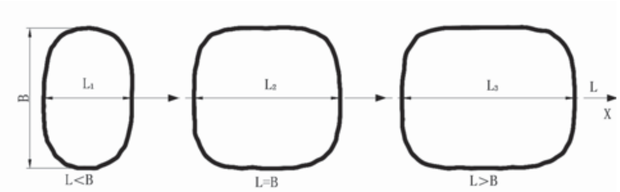

Figure 1—Changes in the shape of the surface subsidence basin (plan view) with changes in the ratio of working face length (*B*) to working face advance (*L*)

therefore it is beneficial to understand its spatial and temporal evolution by adopting the combined research models of excavation, strata movement, and surface subsidence. Moreover, studying the development and changing trends of surface movement and the subsidence field during coal mining has great scientific significance with respect to responsible exploitation of underground mineral resources and reduction of surface subsidence and environmental damage.

Structures of surface subsidence

Underground engineers assume different structural models and propose diverse structural hypotheses of surface subsidence based on their own research and practical experience. A surface subsidence basin can take three main forms, as shown in Figure 1 in plan view, depending on the ratio of the length of the working face (*B*) to the advance distance (*L*). If the distance of advance of the working face (*L*) is less than the length, the surface subsidence basin is elliptical. As the distance of advance of working face increases, the shape of the surface subsidence is transformed from elliptical to circular when *L* is equal to *B*, and then back to an ellipse when *L* exceeds *B*.

The maximum surface subsidence occurs in the middle of the goaf. Therefore, the surface displacement curve, which is shown in Figure 2, can be obtained by taking the distance of advance of the working face as the *X* axis and the central axis (Y axis) of the surface subsidence basin as a vertical section.

Surface subsidence changes as the coal seam is mined, thus the surface subsidence curve differs with the intensity of excavation. The entire process of surface subsidence can be divided into stages from W1 to W12, as shown in Figure 2. According to the surface subsidence value and characteristics of the curve, the evolution of surface subsidence can also be divided into four major stages: the micro-change stage, the development of surface subsidence, formation of a moving subsidence field, and dynamic balance.

- The first stage (I) represents micro-changes, represented by curves W1, W2, and W3 in Figure 2. If the advance distance of the working face is less than H/π, then surface subsidence is not significant. An advance distance of H/π can therefore be considered as heralding the onset of surface subsidence.
- The second stage (II) is the development of surface subsidence, represented by curves W4, W5, and W6. In this stage, the advance distance usually varies from H/π to $2H/\pi$. The rate of surface subsidence is greater than that in stage I; therefore, surface subsidence increases significantly as excavation progresses. An advance distance of $2H/\pi$ can be considered as the critical point, at which the surface enters into full subsidence.
- When the advance distance increases from $2H/\pi$ to $4H/\pi$, the moving subsidence field can be regarded as being in the third stage (III) in the overall process of surface subsidence, such as represented by the curves W7, W8, and W9. In this stage, the curve of surface

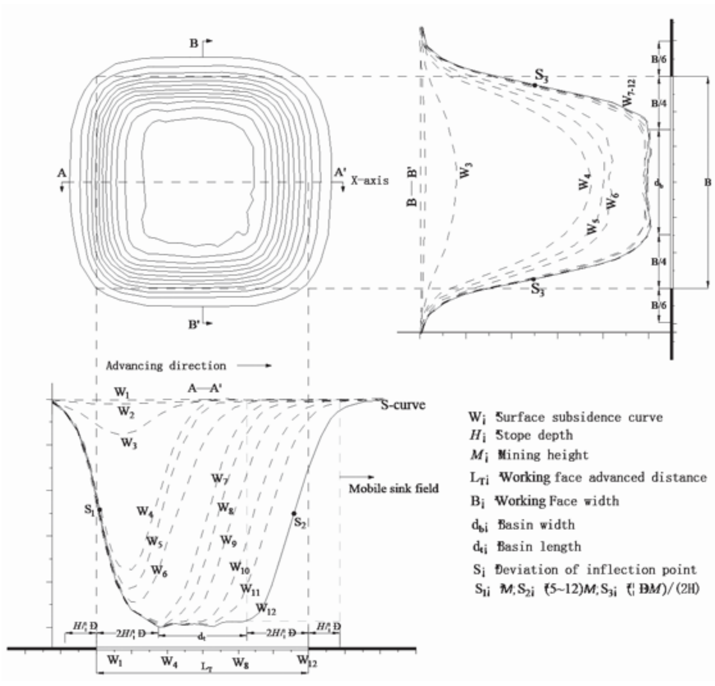

Figure 2—Evolution of surface subsidence

subsidence behind the goaf is no longer affected by mining and is stable on the goaf side. Moreover, if the deviation of the inflection point of curve S1 is equal to the mining height (M), a moving subsidence field in front of the goaf is gradually formed until the advance distance increases to $4H/\pi$, at which time a basin begins to form.

- If the advance distance exceeds $4H/\pi$, the dynamic balance stage (IV) is established, represented by the curves W10, W11, and W12. The moving subsidence field of the working face continuously moves forward as mining progresses. The area distribution is shown as a red dotted outline in Figure 2. In this stage, surface subsidence reaches full subsidence and the basin begins to sink. The length and width of the basin can be calculated by $d_t = L_T - 4H/\pi$ and $d_b = \max(B - H, B/2)$ respectively, in the direction of the working face arrangement. The deviation of the inflection point of the lateral surface subsidence curve, which can be calculated from $S_3 = \pi BM/(2H)$, is stable on the goaf side. The inflection point of the surface subsidence curve ahead of the working face can be calculated from $S_2 = (5\text{~}12)M$. The inflection point fluctuates on the goaf side as the working face advances.

A magnification of the curve representing the moving subsidence field is shown in Figure 3. This can be regarded as an S-curve distribution and conforms to the DoseResp curve characteristics.

The formula of this curve is given by

$$y = A1 + \frac{A2 - A1}{1 + 10^{(LOGx0 - x)p}}$$

where $A1$ represents the maximum value of surface subsidence, $A2$ is the subsidence value of the surface boundary point, LOGx0 is the deviation of the inflection point, and p is the slope of the curve. Parameters $A1$, $A2$, and LOGx0 can therefore be used to characterize the evolution characteristics of surface subsidence.

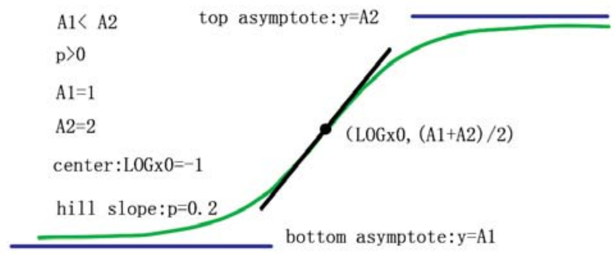

Figure 3—Characteristics of the DoseResp curve

Numerical simulation model

The geological and mining technology conditions of the 42108 working face of Liangshuijing coal mine, China, were combined with borehole data to simulate the process of overall rock movement from open-off mining to full subsidence. The three-dimensional discrete element simulation software *3DEC* was employed. The numerical simulation model is shown in Figure 4.

The length and width of the model were 500 m and 400 m, respectively. The burial depth of the coal seam was 120 m. The section is shown in Figure 5, indicating that there are seven lithological types, from top to bottom: aeolian sand (20 m), mild clay (32 m), medium coarse-grained sandstone (20 m), medium-grained sandstone (24 m), fine-grained sandstone (7 m), coal seam (3 m), and siltstone (10 m). The strata overlying the coal seam have a total thickness of 106 m. The lithology of the roof is mainly siltstone and fine sandstone, medium-grained sandstone, and mudstone; the immediate roof is mudstone. According to this lithology, the roof can be regard as being of medium stability (Class II) and of Type 2. The lithology of the floor is mainly siltstone, fine-grained sandstone, and mudstone.

The physical and mechanical parameters of these rocks were evaluated using laboratory tests, and the values

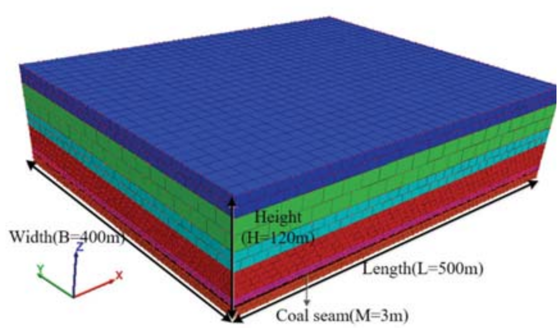

Figure 4—Schematic of numerical simulation model

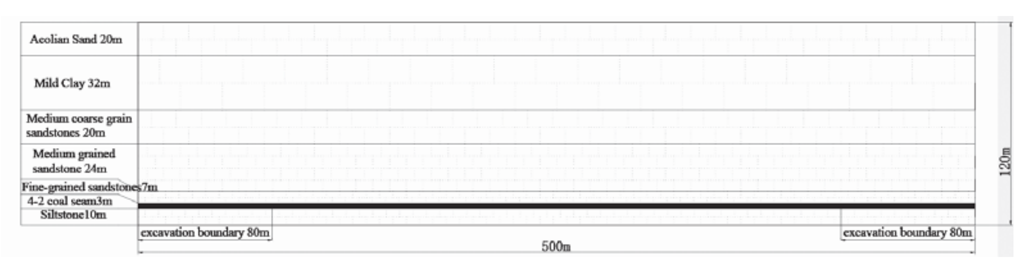

Figure 5 – Lithology of strike section

Table I

Physical and mechanical parameters of strata

Rock stratum		Thickness (m)	Density (kg/m³)	Bulk modulus (GPa)	Shear modulus (GPa)	Cohesion (MPa)	Internal friction angle (°)	Tensile strength (MPa)
Roof	Aeolian sand	20	2635	33	32	2	38	1
	Mild clay	36	1370	8	7.3	0.4	20	0.3
	Medium -coarse grained sandstones	20	2635	20	10	0.1	18	0.1
	Medium -grained sandstone	24	2560	10	10	0.4	19	0.6
	Fine-grained sandstones	7	2635	10	10	0.8	20	0.9
Coal seam	4-2 coal seam	3	2220	8	4	0.1	15	0.4
Floor	Siltstone	10	2560	8	4	0.1	15	0.04

employed in the numerical simulation model are shown in Table I. The Mohr–Coulomb failure criterion was adopted.

According to Peng (2006), there is a critical value of the working face width (B) that is linearly related to mining depth (H) when the ground surface is fully subsided. Therefore: $B = 100 + 1.048H = 212$ m. Because the length of this model was 500 m and the width of the boundary coal pillars on both sides was 80 m, the advance distance was 340 m, which is approximately π times the mining depth (H). From the above result, it can be seen that the length of the working face was larger than the critical length of full mining.

Surface subsidence parameter analysis

Analysis of trends in inflection point

The concave (internal) and convex (external) portions of the surface subsidence curves are separated by inflection points. These are situated where the slope of the surface subsidence curve reaches a maximum and the curvature is zero. The inflection point occurs at the junction of the coal body and goaf under ideal conditions; in fact, the inflection point position varies as the stope advances and finally stabilizes at the side of the goaf. Therefore, to discuss changes in the inflection point of the subsidence curve in detail, the front side of the advancing goaf was defined as the front inflection point of the surface subsidence curve; similarly, the back and lateral side of the advancing goaf were defined as the back and lateral inflection points, respectively. Changes in the inflection point of the surface subsidence curve as the working face advances are shown in Figure 6.

The red curve in Figure 6 indicates the change of the inflection point in front of the goaf with advance of the working face. Overall, the location of the inflection point at the side of the goaf showed an approximately linear relationship with the advance distance of the working face during the periods of micro-change, development, and formation of the movement subsidence field. However, when the advance distance exceeded $4H/\pi$, which represents the dynamic balance stage, the location of the inflection point was in homeostasis and fluctuated between $5M$ abd $12M$ on the goaf side due to the influence of the moving abutment pressure in front of the working face.

Similarly, the black curve illustrates the change of the inflection point at the back of the goaf with advance of the

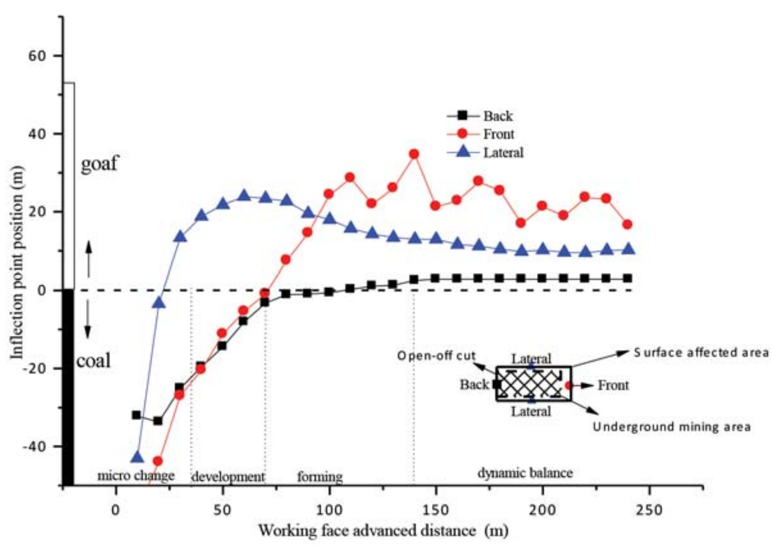

Figure 6—Changes in the location of inflection points with advance distance of the working face (*L*). Width of working face (*B*) 240 m; burial depth (*H*) 120 m; mining height (*M*) 3 m

working face. The starting position of the inflection point was ten times the mining height on the side of the coal body behind the open-off cut. As the working face advanced, the inflection point became offset to the side of the goaf. When movement of the subsidence field remained at the stage of micro-change and development (*i.e.*, the advance distance was less than $2H/\pi$), the location of the inflection point was always stable at the side of the coal body; its location transfers to the side of the goaf during the stage of movement of the stress field. Finally, when the advance distance exceeded $4H/\pi$, the inflection point position stabilized at 3 m on the side of the goaf in the dynamic equilibrium stage.

The blue curve shows changes of the inflection point lateral to the goaf with advance of the working face. Because the length of the working face was much larger than the advance distance in the initial stage, the deflection velocity of the lateral region was obviously greater than that of the front and back, thus the inflection point was transferred from the coal body to the goaf in the micro-change stage, and then to deep in the goaf in the development stage. Finally, the location of the inflection point returned some distance and stabilized at 7 m, which can be calculated by the formula $(\pi BM)/(2H)$.

Analysis of trends in the boundary point position and maximum value of surface subsidence

The process of surface subsidence caused by underground mining is a complex space-time phenomenon. In theory, the amount of subsidence is equal to the increase in underground space; in fact, surface subsidence does not have the same value at different positions of the goaf due to the continuous advance of the working face. The changes in the amount of subsidence of the boundary point and the maximum subsidence of the surface are shown in Figure 7 from the open-off cut to a position at which the advance distance of the working face is equal to its length ($L=B$).

The maximum subsidence of the surface caused by excavation is shown as the green and pink curves in Figure 7. These curves show that the peak value of subsidence bore little relation to the length of the working face and the amount of subsidence increased with advance of the mining distance. The peak value of surface subsidence no longer increased and began to stabilize when the advance distance reached $4H/\pi$ and movement of the subsidence field occurred. Similarly, the subsidence increased with working face mining in the stages of micro-change and development to the back and front boundary points of the excavation. However, the back boundary point was static, so the subsidence increased to a certain extent and was then no longer influenced by mining when the advance distance exceeded $2H/\pi$, which meant that the initial subsidence field had formed. For the front boundary point, the next value fluctuated and the subsidence value was always lower than that of the rear value because of moving abutment pressure.

Regarding the lateral boundary settlement, there was no change when the advance distance reached 160 m, which was less than the empirically calculated critical value of about 240 m, because the length of working face (240 m) was larger than $4H/\pi$. Therefore, if the size of the excavation is less than $2H/\pi$, the ground surface does not form a movement subsidence field; if the excavation size is less than $4H/\pi$, a movement subsidence field can form. However, the working face can reach the full mining extent and the moving stress field can enter the dynamic balance stage without the advance distance reaching the length of the working face once the excavation size exceeds $4H/\pi$.

Analysis of trends in slope of surface subsidence curve

The distribution and process of change of a surface subsidence curve caused by coal seam mining can be represented by the slope of the subsidence curve. The changes in slope of the surface subsidence boundary curve about the working face are shown in Figure 8 for the open-off cut to an advance distance of the working face equal to its length.

The slopes on the front, back, and lateral side of the goaf can indicate changes in the surface subsidence curve. The curve obviously underwent fluctuation, which meant that

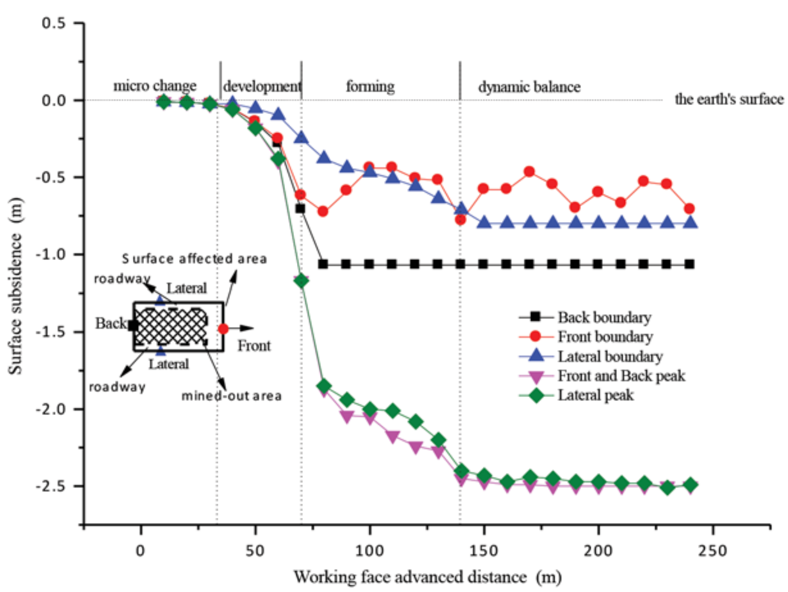

Figure 7 – Change in excavation boundary point and maximum subsidence point with advance distance of the working face (*L*). Width of working face (*B*) 240 m; burial depth (*H*) 120 m; mining height (*M*) 3 m

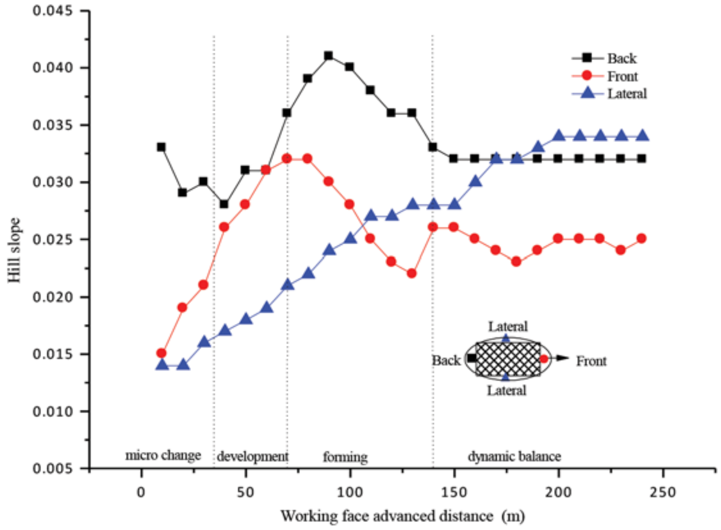

Figure 8—Changes in slope of surface subsidence curve with advance distance of working face. Width of working face (*B*) 240 m; burial depth (*H*) 120 m; mining height (*M*) 3 m

surface subsidence exhibited a non-uniform velocity variation as the working face advanced. When the width of the working face exceeded $4H/\pi$, the slope of the lateral surface subsidence curve always increased until it stabilized.

The slope of the subsidence curve is affected by mining and can fluctuate in the micro-variable stage. It then constantly increases in the development stage, finally reaching a peak value before decreasing again during the stage of subsidence field formation. The slope therefore displays significant variation when the advance distance is $2H/\pi$. With continuous advance of the working face, the slope decreased until the advance distance equalled $4H/\pi$, at which point the slope tended to stabilize. The slope of the subsidence curve on the front side of the surface rises sharply from the open-off cut, reaches a peak value when the advance distance is $2H/\pi$, then drops continuously until the advance is $4H/\pi$ where it reaches a local minimum; however, it begins to increase again during the full mining stage. In summary, the slope of the front subsidence curve is in a weak fluctuation and cannot be stabilized due to the influence of the working face excavation. The slope of the surface subsidence curve at the back of the goaf is always greater than that of the lateral side, which indicates that the slope in the advancing direction is always larger than that of inclination.

Conclusion

Surface subsidence is a gradual process of formation and development, the characteristics of which are related to burial depth and the dimensions of the excavation. The distances of influence of the movement subsidence field at the front of the coal body and the side of goaf are H/π and $2H/\pi$, respectively. The width of the basin can be calculated by reducing the working face advance distance by $4H/\pi$. According to the ratio of burial depth to advance distance and the characteristics of the movement subsidence field, the evolution of the surface subsidence curve can be divided into four stages: the micro-change stage, the development of surface subsidence, formation of a moving subsidence field, and dynamic balance. When the burial depth, width of the working face, and advance distance are designated *H, B,* and *L,* respectively, the distance of the micro-change stage varies from zero to H/π, that of the development of surface subsidence varies from H/π to $2H/\pi$, the formation of the moving subsidence field varies from $2H/\pi$ to $4H/\pi$, and the range of the dynamic balance stage exceeds $4H/\pi$. The width of the basin that is formed by surface subsidence is the maximum value of both $(B - H)$ and $B/2$ or $(L - 4H/\pi)$. These results can provide scientific guidance for green mining and ecological mitigation and control.

Acknowledgment

This research is funded by the National Key Basic Research Program (2016YFC0501100). The authors are grateful to their State Key Laboratory of Water Resource Protection and Utilization in Coal Mining for their help and Kathryn Sole, PhD, for editing the English.

References

China National Coal Association. 2018. Annual report on China's coal industry in 2017.

Choi, D.S. and Dahl, H.D. 1981. Measurement and prediction of mine subsidence over room and pillar in three dimensions. *Proceedings of the Workshop on Subsidence due to Underground Mining*. Peng, S.S. (ed.). West Virginia University, Morgantown, WV. pp. 34–47.

Cui, X.M, and Deng, K.Z. 2017. Research review of predicting theory and method for coal mining subsidence. *Coal Science and Technology*, vol. 45. pp. 160–169.

Hu, H.F. 2012. Research on surface subsidence regularity and prediction under composite media with different thickness rations of loose bedrock. PhD thesis, Taiyuan University of Technology.

Kratzch, H 1983. Mining Subsidence Engineering. Springer-Verlag, Berlin, Heidelberg.

Liu, Z. 2008. Research on the deformation rule of surface movement caused by mining under the conditions of thick alluvium and hard solid rock. Master's thesis, Xi`an University of Science and Technology.

Lu, T.T. 2015. Surface change detection using InSAR technology. Master's thesis, Chang'an University.

Ma, F.H. and Yang, F. 2001. Research on numerical simulation of stratum subsidence. *Journal of Liaoning Technical University Natural Science,* vol. 20. pp. 257–261.

Peng, S.S. 2011. Longwall Mining, 2nd edn. Science Press, Beijing. ◆